

## Review Article

# Biomechanical Macromodel for Estimating Loads in Three Segments of the Spine during Lifting Tasks

Marcelo La Torre<sup>\*1,2</sup>, Débora Cantergi<sup>3</sup>, Cláudia Tarragô Candotti<sup>3</sup>, Jefferson Fagundes Loss<sup>3</sup>

<sup>1</sup>Unisinos - Vale do Rio dos Sinos University, São Leopoldo, Brazil

<sup>2</sup>University of Caxias do Sul, Caxias do Sul, Brazil

<sup>3</sup>Federal University of Rio Grande do Sul, Porto Alegre, Brazil

**\*Corresponding author:** Marcelo La Torre, Edmundo Bastian 333 AP 801, Cristo redentor 91040-050, Porto Alegre, Brazil.  
Tel:(51) 35911122; E-mail: marcelotorre@unisinos.br

**Citation:** Torre ML, Cantergi D, Candotti CT, Loss JF (2017) Biomechanical Macromodel for Estimating Loads in Three Segments of the Spine During Lifting Tasks. J Orthop Ther: JORT-134. DOI: 10.29011/JORT-134.000034

**Received Date:** 20 April, 2017; **Accepted Date:** 9 May, 2017; **Published Date:** 16 May, 2017

## Abstract

Among daily life activities, lifting an object from the floor imposes some of the highest loads on the lumbar spine. Several biomechanical macromodels are found in literature that attempt to assess the loads imposed on the spine. However, most models consider the vertebral spine to be a single rigid segment. This study aimed to develop a biomechanical macromodel that divides the spine into three mobile segments. The macromodel was composed of a linked 16 segment model associated with an inverse dynamics solution and a muscular and articular force distribution model. The model was evaluated using one subject, who performed two lifting techniques (stoop and squat), and demonstrated internal coherence. The maximum forces estimated for each trunk segment during stoop were 3594 N for the lower trunk, 3200 N for the medium trunk, and 1730 N for the superior trunk during load handling; during squat, the maximum estimated forces were 2700 N for the lower trunk, 2455 N for the medium trunk, and 1519 N for the superior trunk during load handling.

**Keywords:** Inverse Dynamics; Loads; Lifting; Model; Spine

## Introduction

Loads imposed on the body during daily life activities and sports events are the interest of several biomechanical studies [1-5], with lifting activities receiving particular interest [6]. Among daily life activities, lifting an object from the floor imposes some of the highest loads on the lumbar spine [7,8]. Because of the high loads associated with this activity, lifting is generally related to factors generating lumbar disorders [9-11]. According to Cheng et al. [12], high compressive loads on the lumbar vertebrae are considered to be a main cause of most lumbar disorders. Assessing loads imposed on the spinal structure during lifting tasks is mainly achieved in two ways:

- Direct Measurement, which is limited due to technological and ethical issues [5,7,13]; and
- Indirect Analytical Procedure, which uses external measures and modeling for estimating internal forces in a non-invasive manner [3,14-16].

Several biomechanical macromodels have been reported in the literature [12,17-20]. Such macromodels consist of a Linked Segment Model (LSM) and a distribution model. Linked segmental models are associated with inverse dynamics technique, and are used to calculate reaction forces and net proximal moments in the joint of interest. Distribution models divide the reaction forces and net proximal moments among muscular and articular components of the joints.

The first models to use indirect measures to simulate postures and movements for estimating lumbar spine loads during lifting activities were developed in the 1940s and considered the spine to be a single rigid segment [21]. According to the anthropometric perspective, while the spine may be divided into at least three regions [22], most models still consider the vertebral spine to be a single rigid segment, with a single joint in the lumbar region [12,23-27]. Because the lumbar spine is associated with a high number of disorders, most macromodels in the literature focus only on the lumbar region [28]. However, other regions of the spine also have biomechanical importance. For example, several injuries and deformities are related to the thoracic spine [29]. The

kyphotic curvature in the thoracic region opposes the lumbar lordosis, supports the thoracic region, and helps transfer intra-abdominal pressure to other regions of the body. In order to obtain a more detailed estimate of the net forces and moments involved during lifting tasks, this study aimed to develop a biomechanical macromodel that divides the spine into three mobile segments (upper, medium, and lower trunk) and allows the estimation of internal forces from muscles and joints when lifting a load from the floor with different techniques.

## Methods

### Subject

Input data were obtained from one healthy male subject (23 years old, 175 cm in height, 57.1 kg body weight, hip range of motion over 100 degrees). This project was approved by the ethical committee of the university at which it was developed and the subject gave informed consent to participate in the study.

### Acquisition Procedures and Data Treatment

Two lifting techniques were evaluated:

- Stoop and
- Squat.

Each lifting started and ended in the standing position without the load, and consisted of the lifting and lowering of the load. The lifted load was equivalent to 20% of the subject's body weight. Each technique was repeated twice, in random order, with an interval of five minutes between each repetition. A metronome dictated the speed of execution. The subject performed each lifting in 16 seconds, with four seconds for each phase: lowering the trunk with and without the load, and lifting the trunk with and without the load (Figure 1).



Figure 1: Stoop and Squat Lifting Techniques.

Before data collection, each technique was explained and the subject practiced lifting with the correct speed. Kinematic and kinetic data were collected. Kinematic data was obtained with five digital video cameras at 50 Hz (JVC GR-DVL 9800) using Dvideow software [30,31]. Sixty-nine reflective markers were positioned at anatomical reference points [32,33] and on the lifted load. A global coordinate system was established using a three-dimensional calibrator (Peak Performance 5.3).

Kinetic data was obtained with a strain-gauge force plate at 500 Hz (AMTI OR6-5:50.8 x 46.4 cm) connected to a signal conditioner (Computer Boards, 8-channels CIO-EXP-GP) and a computer with an A/D converter board (Computer Boards, 16 bits). A computer-based Oscillograph and Data Aquisition System-CODAS (DATAQ instruments Inc., Ohio, USA)-was used. The subject was positioned with both feet on the force plate. Signals were considered symmetric, and were divided equally between each foot for the macromodel. Kinematic and kinetic data were processed on Matlab® software. A 4<sup>th</sup> order low-pass Butterworth filter with cut-off frequencies between 5 and 7 Hz was used. Cut-off frequencies were determined using a residual analysis technique [34]. Local reference systems were obtained from non-collinear markers for each body segment [32,33,35]. Kinematic description was performed using Euler angles, according to the recommendations of the International Society of Biomechanics [32,33,36]. Anthropometric parameters were obtained from the literature [37].

### Macromodel

The macromodel was composed of a linked segment model associated with an inverse dynamics solution and a muscular and articular force distribution model. The linked segment model was composed of 16 rigid segments connected by hinge joints (Figure 2).

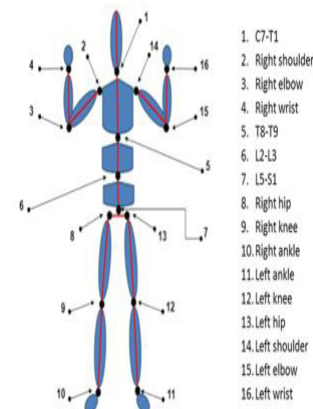


Figure 2: The Link Segment Model Was Composed of 16 Rigid Segments and 16 Joints. The Joints are listed on the Right According to the Number Indicated in the Figure.

Inverse dynamics was used for calculating net forces and moments in each segment's proximal joint [34], expressed in a local reference system, with the origin corresponding to each segment's

center of mass, the y-axis to the segment's longitudinal direction, the x-axis to the anterior-posterior direction, and the z-axis to the lateral-medial direction (Table 1).

Lifting technique	GRS	Mean difference (N)	Standard deviation (N)
Stoop	X	0.81	2.66
	Y	-3.76	6.62
	Z	-3.3	3.17
Squat	X	-0.88	1.61
	Y	-7.17	6.72
	Z	-0.3	3.3

GRS -Global Reference System, With X = Lateral-Medial Axis, Y= Vertical Axis, And Z= Anterior-Posterior Axis.

**Table 1:** Mean Difference and Standard Deviation Between Ground Reaction Forces Calculated Using the Force Plate and Ground Reaction Forces Estimated from the Top-Down Direction in Phases 2 and 3 of the Lifting Technique.

Resultant forces and moments were calculated from two types of assessments:

- Bottom-Up Direction, originating in the foot and ending in the C7-T1 joint, with ground reaction forces as input; and
- Top-Down Direction, originating in the hand segment and ending in the foot, with the external force estimated from the lifted object [25].

Three-dimensional space coordinates originating in the center of the vertebral bodies, and cranial and caudal insertions of 180 muscle slips from the anatomical description given by Stokes and Gardner-Morse [38], were used for defining articular axes and the moment arms associated to each spine region for the distribution model [4]. From the anatomical description, the force action lines of the main muscles responsible for trunk extension were obtained, and three resultant muscle force vectors, one for each trunk segment, were developed. Input for calculating net muscle force vectors were the physiological cross-sectional area and proximal and distal insertion coordinates from the main trunk extension muscles:

- Thoracic Longissimus
- Lumbar Longissimus
- Thoracic Iliocostalis
- Lumbar Iliocostalis
- Quadratus Lumborum
- Thoracic Multifidus
- Lumbar Multifidus.

The weighted average muscle force application point was obtained from the cranial and caudal insertion points of all muscle slips acting on each vertebral level, from T1 to S1, using the physiological

cross-sectional area as a factor. The resulting vertebral level muscle force vectors were then grouped into three trunk segments (Figure 3).

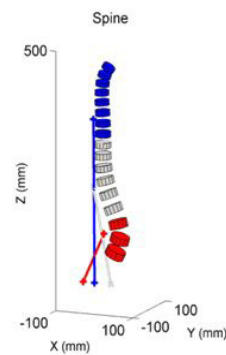


**Figure 3:** Muscle Force Vectors, Point of Application, and Line of Action for the Three Trunk Segments: (1) Upper Trunk: from the C7 Spine Process to the Xiphoid Process (T8); (2) Medium Trunk: The Xiphoid Process to the Belly Line (L2); and (3) Lower Trunk: The Belly Line to A Plane That Crosses The Superior Iliac Crest at 37° Angle (S1).

Data obtained from the link segment model and the force distribution model were used for calculating muscular and articular resultant forces. Resultant moments for each trunk segment were obtained in a top-down direction from the link segment model using Equation 1.

$$MR^i = \sqrt{((M_p^x)^2 + (M_p^y)^2 + (M_p^z)^2)} \quad \text{Equation 1}$$

Where:

$MR^i$  = resultant moment for each segment  $i$ ;

$x$ ,  $y$ , and  $z$  =  $x$ ,  $y$ , and  $z$  components in the local reference system;

$i$  = trunk segments (upper, medium, lower); and

$M_p^i$  = proximal moment obtained in the local reference system for each  $i$  segment.

Muscle force in each trunk segment was calculated using the segment's resultant moment and muscle force vector moment arm, according to Equation 2.

$$F_M^i = \frac{MR^i}{d^{\perp i}} \quad \text{Equation 2}$$

$F_M^i$  = resultant muscle force of  $i$  segment; and

$d^{\perp i}$  = resultant force vector's moment arm of segment  $i$ .

The resultant muscle force incorporated all muscular and articular forces effects. By subtracting the estimated value from the muscle force, the net effect from all articular structures interacting with the joint (ligaments, capsules, cartilage, etc.) was obtained. By definition, the articular force point of application is the center of rotation. Hence, articular force in each trunk segment was calculated using Newton-Euler's first equation.

Equation 3 provides the net articular force in the trunk segments.

$$F_A^i = m_i a_i - (F_M^i + FR_D^i + P^i) \quad \text{Equation 3}$$

$F_A^i$  = resultant articular force of segment  $i$ ;  
 $FR_D^i$  = distal reaction force of segment  $i$ ;  
 $p$  = segment  $i$ 's weight force;  
 $a$  = segment  $i$ 's linear acceleration; and  
 $m$  = segment  $i$ 's mass.

## Results

### Model Evaluation

The link segment model was evaluated using two procedures. First, the vertical component of the ground reaction force, measured using the force plate, was compared to the vertical component of the ground reaction force estimated from the top-down direction (Figure 4).

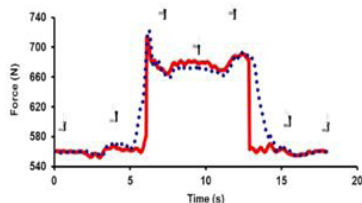


**Figure 4:** The Vertical Component of the Ground Reaction Force Measured Using the Force Plate (Full Line), And the Vertical Component of

the Ground Reaction Force Estimated from the Top-Down Manner (Dotted Line) In the Stoop Lifting Technique. Similar Results Were Found in the Squat Lifting Technique.

Mean differences found between calculated and estimated ground reaction forces during phases 2 and 3 (the phases when the load was being held) for all force components is presented in (Table 2).

Lifting technique	LRS	Mean difference (Nm)	Standard deviation (Nm)
Stoop	X	-0.03	4.19
	Y	1.31	3.95
	Z	14.28	15.22
Squat	X	-0.02	3.83
	Y	-1.39	4.25
	Z	-6.13	8.67

LRS - Local Reference System, With X= Anterior-Posterior Axis, Y= Vertical Axis, And Z = Lateral-Medial Axis.

**Table 2:** Mean Difference and Standard Deviation Between the Lower Trunk Proximal Moment Calculated Using the Bottom-Up and Top-Down Directions in Phases 2 And 3 of the Lifting Technique. Results for the Medium and Upper Trunks Were Similar to These.

The second evaluation procedure compared the proximal moments obtained from the spine joints in the bottom-up direction to those obtained in the top-down direction (Table 3).

Lifting technique	Trunk segment	phase	Maximum FM (N)	Angle(o)	Mínimum FM (N)	Angle(o)	Maximum do FA (N)	Angle(o)	Mínimum do FA (N)	Angle(o)
Stoop	LT	1	2105.9	76	488.1	14	-2462.1	76	-825.8	14
		2 e 3	3594	81	1113.7	18	-4071.9	81	-1572.1	17
	MT	4	2072.9	79	490.7	14	-2419.2	79	-827.5	14
		1	1712.3	76	397.1	14	-2000.5	77	-672.1	14
	MT	2 e 3	3199.8	81	1014.3	18	-3603.9	81	-1409.6	14
Squat	ST	4	1689.6	79	395.2	17	-1971.5	79	-668.8	14
		1	747.1	76	301.8	14	-935.3	76	-485.1	14
	LT	2 e 3	1730.4	81	792.4	18	-2041.2	81	-1096.5	18
		4	772.16	79	250.5	14	-958.6	79	-433.4	14
	MT	1	1503.4	119	498.7	17	-1851.2	118	-833.2	18
		2 e 3	2699.9	114	1240.9	19	-3164.1	114	-1698.4	19
		4	1611.6	117	542	24	-1959.1	117	-878.6	24
		1	1281.5	117	390.7	18	-1562.5	118	-662.9	18
	ST	2 e 3	2455.3	113	1168.7	19	-2854.5	113	-1563.6	19
		4	1373.2	117	423	24	-1653.1	117	-697.2	24
	LT	1	639.5	117	260.1	18	-823.6	117	-441.8	18
		2 e 3	1518.8	113	909	19	-1824.5	113	-1211.7	189
	MT	4	683.9	117	228.2	48	-868.1	117	-408.8	48

LT = Lower Trunk, MT = Medium Trunk, ST = Superior Trunk.

**Table 3:** Maximum and Minimum Muscular and Articular Resultant Forces and the Respective Angle at which they occurred.

### Resultant Muscle Force Vector Moment Arm

The resultant muscle force vector for each trunk segment was calculated with the distribution model being used as input data for the calculation of muscular and articular force. Superior, medium, and lower trunk muscle force vector moment arms were 2.2 cm, 4.8 cm, and 5.4 cm, respectively.

### Muscle and Articular Forces During Lifting

Maximum and minimum muscular and articular resultant forces and the respective angles at which they occurred are presented in (Table 3).

### Discussion

This study aimed to develop a biomechanical macromodel that divides the spine into three mobile segments (upper, medium, and lower trunk) and allows the estimation of internal forces from muscles and joints when lifting a load from the floor with different techniques.

### Model Evaluation

The model was evaluated by comparing the measured and

calculated ground reaction forces and the proximal moments at the L5-S1 joint, calculated in a bottom-up and top-down direction. The mean difference of ground reaction forces was calculated by subtracting the calculated force from the measured force on each axis. This procedure was used by Kingma et al. [25] for validating a link segment model of asymmetric lifting with the squat technique. In the present study, mean differences of  $0.81 \pm 2.66$  N on x-axis,  $3.76 \pm 6.62$  N on y-axis, and  $-3.30 \pm 3.17$  N on z-axis were found when the stoop technique was used, and mean differences of  $-0.88 \pm 1.61$  N on x-axis,  $7.17 \pm 6.72$  N on y-axis, and  $-0.3 \pm 3.3$  N on z-axis were found when squat technique was used. Kingma et al. [25] found values of  $2.0 \pm 2.2$  N on x-axis,  $5.1 \pm 7.1$  N on y-axis, and  $0.4 \pm 2.2$  N on z-axis. In both studies, the largest differences occurred in the y-axis, but in both cases this difference was less than 1% of the mean values obtained in this component. This confirms a good agreement between measured and calculated ground reaction forces. Several studies have compared proximal moments at the L5-S1 joint calculated in the bottom-up and top-down direction (Table 4).

Study	n	Mean Body Weight (kg)	Load (kg)	Lifting task	MP mean difference values (Nm)		
					$x_{Ti}$	$y_{Ti}$	$z_{Ti}$
Present study	1	57.1	11.4	Symmetric Stoop	-0.03	1.31	14.28
				Symmetric Squat	-0.02	-1.49	-6.13
Kingma, et al. [25]	7	76.4	5	Asymmetric Squat	6.6	-2.4	6.1
Plamondon, et al. [18]	3	69	9.6	Asymmetric Squat	4	4	5
Cheng, et al. [12]	1	60	10	Asymmetric Squat	19.2	19	10.8
Larivièrie and Gagnon [39]	1	77	13.6	Symmetric Stoop	-	-	42

LRS-Local Reference System, With X= Anterior-Posterior Axis, Y= Vertical Axis, And Z = Lateral-Medial Axis.

**Table 4:** Mean Difference Values Between Proximal Moments at the L5-S1 Joint Calculated in the Bottom-Up and Top-Down Directions Have Been Used in Several Studies from the Literature.

Although these studies present differences such as the lifting technique used and the percentage of body weight of the lifted load, the mean differences found for proximal moments in the present study are similar to those found in different studies.

### Resulting Muscle Force Vector Moment Arms

While the present study used anthropometric data for estimating moment arms, some studies used MRI or CT techniques for joints that were similar to or near to the ones evaluated in this study (Table 5).

Study	n	Measuring Technique	Level	Moment-Arm (cm)
Present study	1	Estimation	T8-T9	2.2
Present study	1	Estimation	L2-L3	4.8
Present study	1	Estimation	L5-S1	5.4
Jorgensen, et al. [40]	10	MRI	T8	4.9±0.6
Jorgensen, et al. [40]	10	MRI	L2	5.4±0.4
Jorgensen, et al. [40]	10	MRI	L5	6.7±0.7
Jorgensen, et al. [41]	12	MRI	T12-L1	5.1±0.4
Jorgensen, et al. [41]	12	MRI	L2-L3	5.46±0.4
Jorgensen, et al. [41]	12	MRI	L5-S1	6.4±0.4
Wood, et al. [42]	5	MRI	L4-L5	5.3±0.6
Moga, et al. [43]	19	CT	L2-L3	5.3
Moga, et al. [43]	19	CT	L4-L5	5.9

**Table 5:** Muscle Moment Arms Estimated in the Present Study and Measured in Different Studies from the Literature.

The moment arms estimated using the distribution model were similar to those found in the literature when comparing the lower and medium trunks. However, the moment arm obtained for the superior trunk (T8-T9) was 50 to 60% lower than the one presented by Jorgensen, et al. [41]. For this reason, articular and muscular forces were calculated using the moment arms estimated in this study for the lower and medium trunks, and data from Jorgensen, et al. [40] were used for the upper trunk.

### Muscular and Articular Forces Obtained with the Macromodel

Muscular and articular peak forces were higher in all phases and segments when in stoop as opposed to squat. The higher forces (approximately 3600 N) occurred in the lower trunk while the load was being carried. The peak force occurred when the trunk was in a horizontal position and the segment's moment arm was larger. The first attempt we know that tried to develop a theoretical model for calculating muscular and articular forces of the spine based on physical principles was made by Strait, et al. [23]. Their model considered the spine to be a rigid rod with a rotation axis in the L5-S1 joint. Trunk erector muscles were represented by a resulting vector acting on two-thirds of the trunk length from the sacrum in a 120° angle with the spine. Without external load, the calculated trunk muscle force was equivalent to 2000 N, and when an external load of 200 N was considered, the trunk muscle force was 3300

N. Although there is a major difference in their approach, these are similar to the muscular forces found in the lower trunk. Another model that considered the spine as a rigid rod with a rotation axis in the L4-L5 joint was developed by McGill and Norman [24]. They analyzed symmetrical squat lifting of a 27-kg load, which generated a maximum muscular force of 3360 N. The present study differs from theirs in that it considers the spine to be three different segments and for using a lower load (12 kg), which justifies the higher peak found by McGill and Norman [24].

Although models are the most common methodology used for evaluating internal loads, there have been a few studies that were able to measure *in vivo* forces or pressures on the spine during daily life activities, including lifting. In the present study, loads of 800 N to 850 N were found during the standing phase of lifting, without a load. These were similar to values found by Sato, et al. [13], who used a pressure sensor inserted in the L4-L5 joint in the standing position. Sato, et al. [13] also evaluated subjects as they bent forward without a load, and found loads of up to 2100 N. This position may be compared to the lowering and raising of the body without load in phases 1 and 4 of the lifting, which were similar to the results demonstrated during the performance of the stoop lifting technique in the present study. When evaluated with an instrumented vertebral body, which replaced fractured vertebral bodies in five patients (four in the L1 level and one in the L3 level) [8], lifting a load from the floor was the activity with the highest resultant load. The highest forces found were 1649 N among the L1 patients, and 1361 N among the L3 patients. A more recent study from the same group presented data from four male patients (three with L1 level vertebrae replacement and one with L3 level vertebrae replacement) who performed stoop and squat lifting [44] with loads of up to 10.8 kg. In this study, the highest loads measured ranged from 1090 N to 1635 N between patients. The present study evaluated the spine, divided into three segments, articulated in the T8-T9 joint (upper trunk), L2-L3 joint (middle trunk), and L4-L5 joint (lower trunk). The maximum articular forces found in all joints were higher than those reported by Rohlmann, et al. [8] and Dreischarf et al. [44]. One possible reason for this difference was the configuration of the instrumented vertebral body, which included the use of internal spinal fixation devices. The authors acknowledge that the measured load does not represent the total spinal load, as it was shared with the internal spinal fixation device and other structures [5].

Articular force was estimated at the L5-S1 joint by three modeling techniques, including a double linear optimization procedure [39]. While lifting 12 kg using the stoop technique in a range of motion of 45°, articular forces of  $3325 \pm 372$  N were found. This value is lower than the one found for this joint (4071.9 N) in the present study; however, this articular force occurred in a position with about 80° of hip flexion. A more horizontal trunk

position will present a larger moment arm and, consequently, a higher moment from the trunk segment, which may explain the higher values in the present study. When working with biomechanical models, simplifications and limitations are inherent to the attempted representation. Among the limitations of the present study was the use of only one force plate, the non-identification of the sacrum's orientation, and the reduced number of cameras. The main limitation was the requirement to maintain spine curvatures during task execution, because the moment arm calculations are based only in the orthostatic position. Another important limitation was the impossibility of comparing the results to an actual value for each variable.

## Conclusion

The model developed in this study demonstrates internal coherence, as shown by the similarity of results obtained in both bottom-up and top-down direction. It was not possible to compare the results to a "Golden Pattern", but they were similar to what was expected in the analyzed situations. The maximum forces estimated for each trunk segment during stoop were 3594 N for the lower trunk, 3200 N for the medium trunk, and 1730 N for the superior trunk during load handling; during squat, the maximum estimated forces were 2700 N for the lower trunk, 2455 N for the medium trunk, and 1519 N for the superior trunk during load handling.

## References

1. Granata KP, Marras WS (1995) An EMG-assisted model of trunk loading during free-dynamic lifting. *J Biomech* 28: 1309-1317.
2. van den Bogert AJ, Read L, Nigg BM (1996) A method for inverse dynamic analysis using accelerometry. *J Biomech* 29: 949-954.
3. Søgaard K, Laursen B, Jensen BR, Sjøgaard G (2001) Dynamic loads on the upper extremities during two different floor cleaning methods. *Clin Biomech* 16: 866-879.
4. Erdemir A, McLean S, Herzog W, van den Bogert AJ (2007) Model-based estimation of muscle forces exerted during movements. *Clin Biomech* 22: 131-154.
5. Rohlmann A, Graichen F, Bender A, Kayser R, Bergmann G (2008) Loads on a telemeterized vertebral body replacement measured in three patients within the first postoperative month. *Clin Biomech* 23: 147-158.
6. Rohlmann A, Zander T, Graichen F, Bergmann G (2013) Lifting up and laying down a weight causes high spinal loads. *J Biomech* 46: 511-514.
7. Wilke HJ, Neef P, Caimi M, Hoogland T, Claes LE (1999) New in vivo measurements of pressures in the intervertebral disc in daily life. *Spine* 24: 755-762.
8. Rohlmann A, Pohl D, Bender A, Graichen F, Dymke J, et al. (2014) Activities of everyday life with high spinal loads. *PloS one* 9: p.e98510.
9. Ferguson SA, Marras WS (1997) A literature review of low back disorder surveillance measures and risk factors. *Clin Biomech* 12: 211-226.
10. Kuiper JI, Burdorf A, Verbeek JH, Frings-Dresen MH, van der Beek AJ, et al. (1999) Epidemiologic evidence on manual materials handling as a risk factor for back disorders: a systematic review. *International Journal of Industrial Ergonomics* 24: 389-404.
11. Nachemson A (1999) Back pain: delimiting the problem in the next millennium. *International journal of Law and Psychiatry* 22: 473-490.
12. Cheng CK, Chen HH, Kuo HH, Lee CL, Chen WJ, et al. (1998) A three-dimensional mathematical model for predicting spinal joint force distribution during manual liftings. *Clin Biomech* 13: S59-S64.
13. Sato K, Kikuchi S, Yonezawa T (1999) In vivo intradiscal pressure measurement in healthy individuals and in patients with ongoing back problems. *Spine* 24: 2468-2474.
14. Plamondon A, Gagnon M, Gravel D (1995) Moments at the L 5/S 1 joint during asymmetrical lifting: effects of different load trajectories and initial load positions. *Clin Biomech* 10: 128-136.
15. Wilson DJ, Hickey KM, Gorham JL, Childers MK (1997) Lumbar spinal moments in chronic back pain patients during supported lifting: A dynamic analysis. *Arch Phys Med Rehabil* 78: 967-972.
16. Arjmand N, Shirazi-Adl A, Parnianpour M (2008) Trunk biomechanics during maximum isometric axial torque exertions in upright standing. *Clin Biomech* 23: 969-978.
17. Delleman NJ, Drost MR, Huson A (1992) Value of biomechanical macromodels as suitable tools for the prevention of work-related low back problems. *Clin Biomech* 7: 138-148.
18. Plamondon A, Gagnon M, Desjardins P (1996) Validation of two 3-D segment models to calculate the net reaction forces and moments at the L5/S1 joint in lifting. *Clin Biomech* 11: 101-110.
19. Amarantini D, Martin L (2004) A method to combine numerical optimization and EMG data for the estimation of joint moments under dynamic conditions. *J Biomech* 37: 1393-1404.
20. Arjmand N, Gagnon D, Plamondon A, Shirazi-Adl A, Larivière C (2009) Comparison of trunk muscle forces and spinal loads estimated by two biomechanical models. *Clin Biomech* 24: 533-541.
21. Wilke HJ, Neef P, Hinz B, Seidel H, Claes L (2001) Intradiscal pressure together with anthropometric data—a data set for the validation of models. *Clin Biomech* 16: S111-S126.
22. Zatsiorsky VM (2002) Kinetics of human motion. Human Kinetics, Champaign, IL.
23. Strait LA, Inman VT, Ralston HJ (1947) Sample illustrations of physical principles selected from physiology and medicine. *American Journal of Physics* 15: 375-382.
24. McGill SM, Norman RW (1986) Partitioning of the L4-L5 Dynamic Moment into Disk, Ligamentous, and Muscular Components during Lifting. *Spine* 11: 666-678.
25. Kingma I, de Looze MP, Toussaint HM, Klijnsma HG, Bruijnen TB (1996) Validation of a full body 3-D dynamic linked segment model. *Human Movement Science* 15: 833-860.
26. Larivière C, Gagnon D, Gravel D, Arsenault AB, Dumas JP, et al. (2001) A triaxial dynamometer to monitor lateral bending and axial rotation moments during static trunk extension efforts. *Clin Biomech* 16: 80-83.

27. Daggfeldt K, Thorstensson A (2003) The mechanics of back-extensor torque production about the lumbar spine. *J Biomech* 36: 815-825.
28. Dreischarf M, Zander T, Shirazi-Adl A, Puttlitz CM, Adam CJ, et al. (2014) Comparison of eight published static finite element models of the intact lumbar spine: Predictive power of models improves when combined together. *J Biomech* 47: 1757-1766.
29. Polga DJ, Beaubien BP, Kallemeier PM, Schellhas KP, Lew WD, et al. (2004) Measurement of in vivo intradiscal pressure in healthy thoracic intervertebral discs. *Spine* 29: 1320-1324.
30. Barros RD, Brenzikofer R, Leite NJ, Figueiroa PJ (1999) Desenvolvimento e avaliação de um sistema para análise cinemática tridimensional de movimentos humanos. *Revista Brasileira de Engenharia Biomédica* 15 : 79-86.
31. Figueiroa PJ, Leite NJ, Barros RM (2003) A flexible software for tracking of markers used in human motion analysis. *Computer methods and programs in biomedicine* 72: 155-165.
32. Wu G, Siegler S, Allard P, Kirtley C, Leardini A, et al. (2002) ISB recommendation on definitions of joint coordinate system of various joints for the reporting of human joint motion-part I: ankle, hip, and spine. *J Biomech* 35: 543-548.
33. Wu G, van-der-Helm FC, Veeger HD, Makhous M, Roy PV, et al. (2005) ISB recommendation on definitions of joint coordinate systems of various joints for the reporting of human joint motion—Part II: shoulder, elbow, wrist and hand. *J Biomech* 38: 981-992.
34. Winter DA (2009) Biomechanics and motor control of human movement. In:4, John Wiley & Sons, New York.
35. Vaughan CL, Davis BL, O'connor JC (1992) Dynamics of human gait. Human Kinetics Publishers, Champaign, IL : 88-92.
36. Wu G, Cavanagh PR (1995) ISB recommendations for standardization in the reporting of kinematic data. *J Biomech* 28: 1257-1261.
37. DeLeva P (1996) Adjustments to Zatsiorsky-Seluyanov's segment inertia parameters. *J Biomech* 29: 1223-1230.
38. Stokes IA, Gardner-Morse M (1999) Quantitative anatomy of the lumbar musculature. *J Biomechanics* 32 : 311-316.
39. Larivière C, Gagnon D (1998) Comparison between two dynamic methods to estimate triaxial net reaction moments at the L5/S1 joint during lifting. *Clin Biomech* 13: 36-47.
40. Jorgensen MJ, Marras WS, Granata KP, Wiand JW (2001) MRI-derived moment-arms of the female and male spine loading muscles. *Clin Biomech* 16: 182-193.
41. Jorgensen MJ, Marras WS, Gupta P, Waters TR (2003) Effect of torso flexion on the lumbar torso extensor muscle sagittal plane moment arms. *Spine* 3: 363-369.
42. Wood S, Pearsall DJ, Ross R, Reid JG (1996) Trunk muscle parameters determined from MRI for lean to obese males. *Clin Biomech* 11: 139-144.
43. Moga PJ, Erig M, Nussbaum MA (1993) Torso muscle moment arms at intervertebral levels T10 through L5 from CT scans on eleven male and eight female subjects. *Spine* 18 : 2305-2309.
44. Dreischarf M, Rohlmann A, Graichen F, Bergmann G, Schmidt H (2015) In vivo loads on a vertebral body replacement during different lifting techniques. *J Biomech* 49: 890-895.